Journal of Nuclear Materials 176 & 177 (1990) 926–934
North-Holland

Neutral gas temperature and densities in the divertor region and pump duct of ITER

D.N. Ruzic
University of Illinois, Department of Nuclear Engineering, 103 South Goodwin Avenue, Urbana, IL 61801, USA

K.A. Werley
Los Alamos National Laboratory, Los Alamos, NM 87545, USA

S.A. Cohen
Princeton Plasma Physics Laboratory, P.O. Box 451, Princeton NJ 08543, USA

A 2-D Monte-Carlo simulation of the neutral atom densities in the divertor, divertor throat and pump duct of ITER was made using the DEGAS code. Plasma conditions in the scrape-off layer and region near the separatrix were modeled using the B2 plasma transport code. Wall reflection coefficients including the effect of realistic surface roughness were determined by using the fractal TRIM code. The DEGAS and B2 coupling was iterated until a consistent recycling was predicted. Results were obtained for a helium and a deuterium/tritium mixture on seven different ITER divertor throat geometries. Recycling, pumping efficiency ratios, temperatures and densities vary markedly. For example, the helium to hydrogen pumping ratio can show a factor of 2.67 ± 0.53 enhancement over the ratio of helium to hydrogen incident on the divertor plate. If the helium flux profile on the divertor plate is moved outward by 20 cm with respect to the D/T flux profile for this particular geometry, the enhancement increases to 4.36 ± 0.90.

1. Introduction

The International Thermonuclear Experimental Reactor (ITER) tokamak is being designed to achieve long-pulse ignited operation [1]. To achieve those goals, steady state removal of helium ash must be sufficient to maintain a core helium concentration of less than 10% [2] while maintaining a realistic pumping system and minimizing the tritium inventory. Other papers investigate the transport to the separatrix [2]. This paper investigates the effect of the divertor shape and pump duct geometry on deuterium/tritium and helium exhaust.

Two computer codes are coupled in this work. The B2 transport code[3] is a 2-D fluid model which solves the first three coupled moment equations: continuity, momentum balance, and energy balance. Thermal conductivity, diffusivity, viscosity, etc. are taken from recommendations based on a tokamak database. [4] The magnetic flux surfaces for the outboard portion of the double-null ITER configuration are taken as the grid boundaries. The source rate and location for new ions from the divertor plate is determined by specifying a local recycling coefficient along the plate boundary. The B2 code iterates until a self-consistent solution is obtained.

The DEGAS code [5] is a 3-D Monte-Carlo multispecies neutral transport code which contains extensive atomic physics including charge exchange, electron and ion impact ionizations, molecular dissociations etc. Energy and angle-resolved wall reflection coefficients include effects of surface roughness and are taken from fractal TRIM [6,7]. The source rate of neutral atoms comes from the flux of ions to the divertor plate. A particle is no longer followed when it becomes ionized or exits the simulation geometry.

The B2 and DEGAS codes were iterated with a 50–50 D/T plasma until their respective boundary conditions at the divertor plate matched. Then helium was included in DEGAS and several geometries of the diver-

0022-3115/90/$03.50

tor throat were simulated. The next section explains the details of coupling the models and shows their inputs. The resultant neutral densities and recycling coefficients show significant variation as a function of geometry.

2. Models

Input parameters to the B2 code were for the ITER Physics Phase double-null ignited plasma: ohmic heating + auxiliary + alpha power = 218 MW; power entering inner and outer scrape-off-layer = 116 MW; volume averaged electron density = 1.22×10^{20} m^{-3}; electron density at the midplane separatrix = 0.349×10^{20} m^{-3}; Z_{eff} core = 1.66; Z_{eff} midplane = 1.53; plasma current = 22 MA. The B2 geometry is shown in the upper half of fig. 1. The X-point to divertor strikepoint distance is 1.5 m. Though the B2 code is not yet capable of directly simulating a tilted divertor plate, a tilt of 15° is included in the calculations.

The output of the B2 code includes plasma density, electron and ion temperatures in each zone. These values for the lower 24 horizontal by 16 vertical B2 zones were mapped onto the appropriate 24 by 16 zones of the DEGAS geometry (lower half of fig. 1). The distance between the X-point and strike point in the DEGAS simulation was also 1.5 m. The DEGAS geometry was taken directly from the current engineering drawings of the ITER divertor throat. The volume of the individual zones were not preserved during the mapping, but the density, flux and alignment of the zones with the field were maintained. Fig. 2 shows contour plots of the B2 temperature and density outputs as they appear in the realistic (DEGAS) geometry.

In addition to the 2-D plasma profiles, DEGAS needs the ion flux distribution along the divertor plate to act as the neutral source. This is obtained from the temperature and densities of the boundary zones in the B2 simulation and is shown in fig. 3.

Also shown in fig. 3 is the local recycling coefficient used in the B2 code to match the DEGAS results. Several iterations were performed until the net current of atoms across the separatrix in B2 equalled the net loss of atoms to the pump in DEGAS. This iteration was done in two parts. The net loss of particles in B2 is obtained by integrating the flux and the recycling coefficient in fig. 3. For this case, the integrated recycling coefficient equals 0.990. That is, for every 1000 particles that hit the divertor plate, 10 are removed from the B2 simulation. The net loss of particles in DEGAS is obtained by comparing the number of atoms that exit

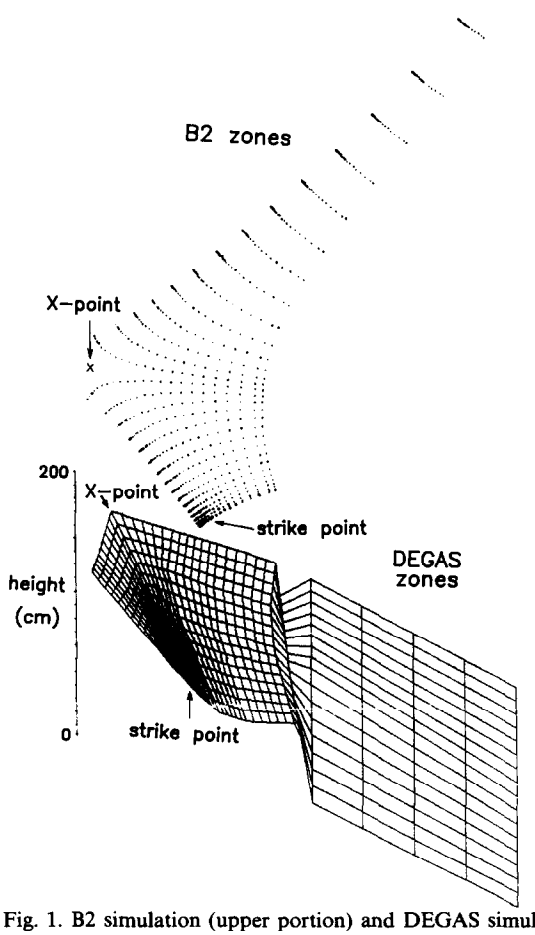

Fig. 1. B2 simulation (upper portion) and DEGAS simulation (lower portion) geometries. The lower 24 horizontal by 16 vertical zones of the B2 simulation were mapped onto 24 by 16 zones of the DEGAS simulation. The X-point to strike point distance was 1.5 m for both simulations.

the simulation through the pump compared to the number that are initiated on the divertor plate.

For this comparison to be valid, 3-dimensional effects must be included. For the B2 code, toroidal symmetry is a valid assumption. However, pump ducts only cover 25% of the ITER design. Further, conductance

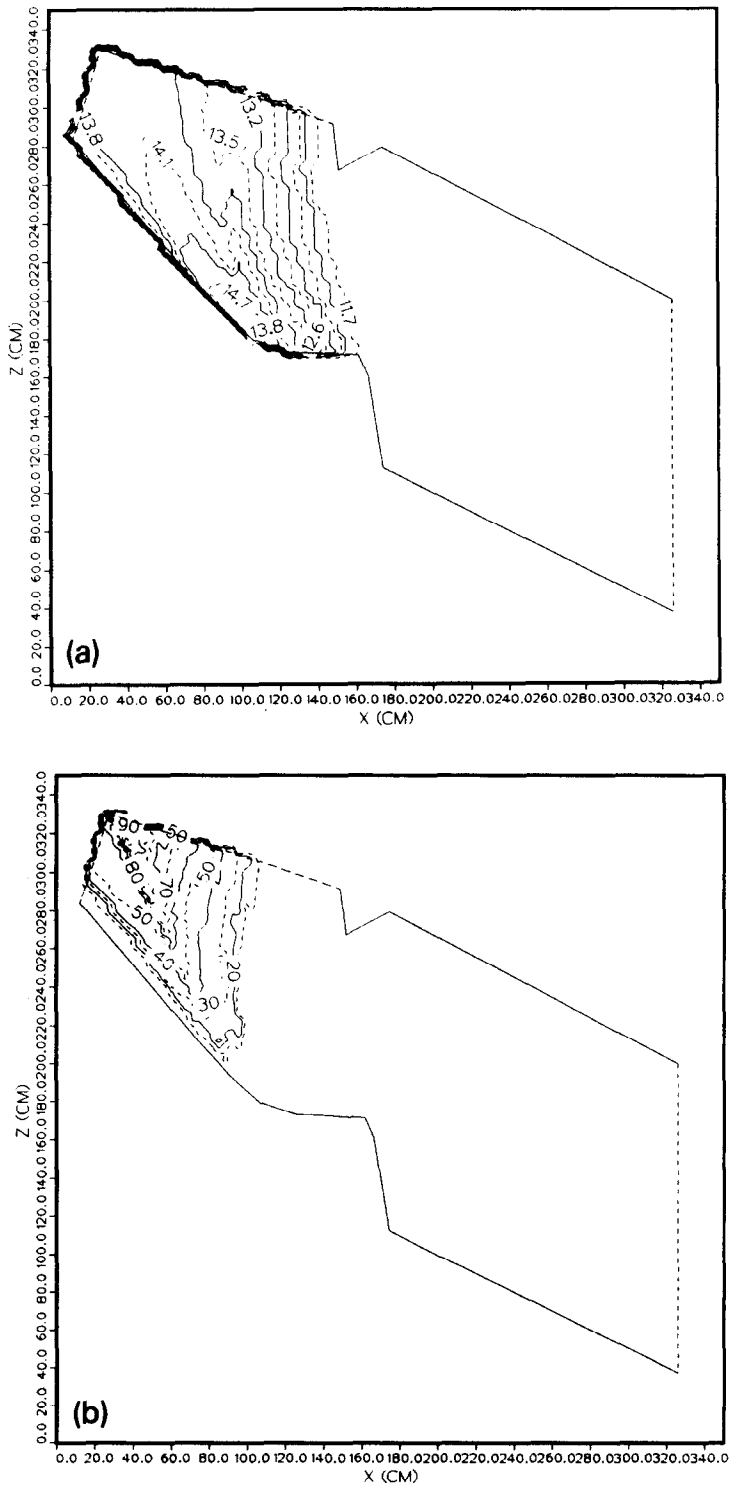

Fig. 2. B2 outputs mapped onto DEGAS zones for (a) electron density, (b) electron temperature, and (c) ion temperature. The contour plot units are cm^{-3} for densities and eV for temperature.

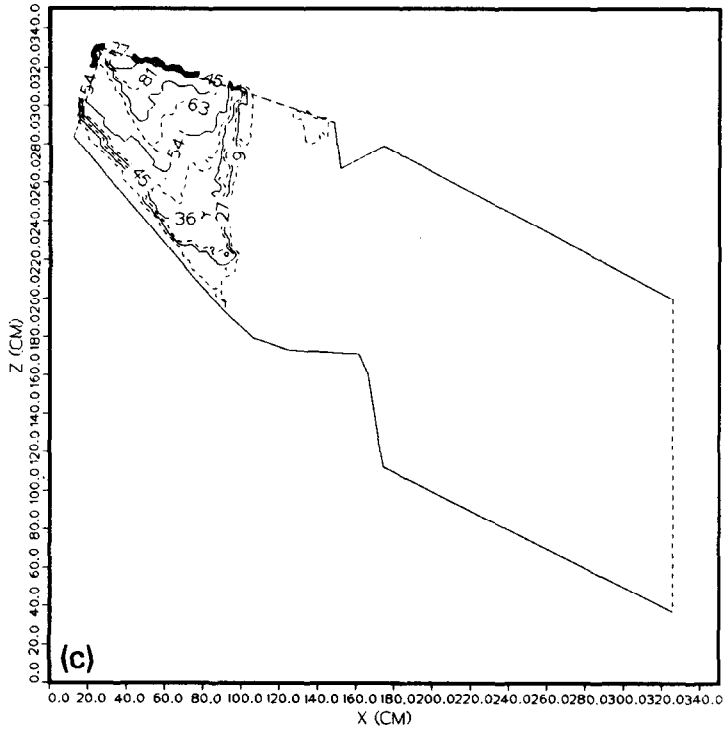

Fig. 2 (continued).

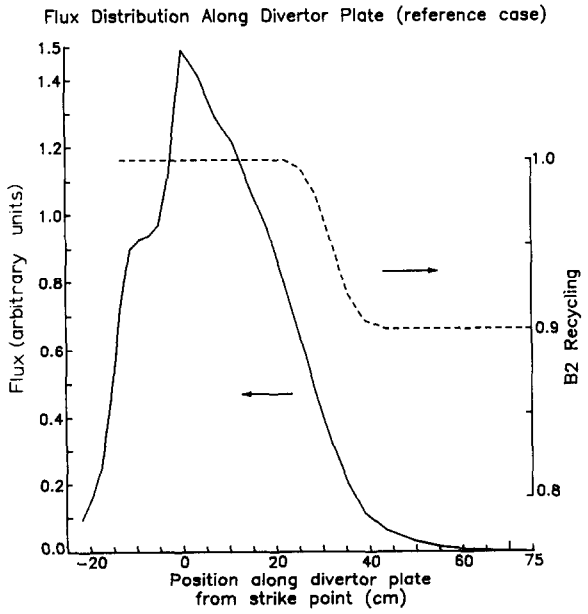

Fig. 3. Flux to the divertor plate and B2 recycling profile needed to match the recycling in the coupled code. The separatrix is at 0 cm on the x-axis.

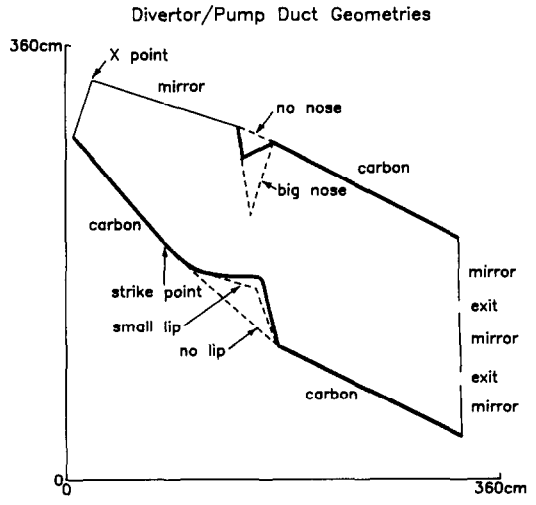

Fig. 4. Divertor and pump duct geometries used in this paper. The albedo of the pump was simulated by having only 12.5% of the pump duct area open on the right hand side of this figure.

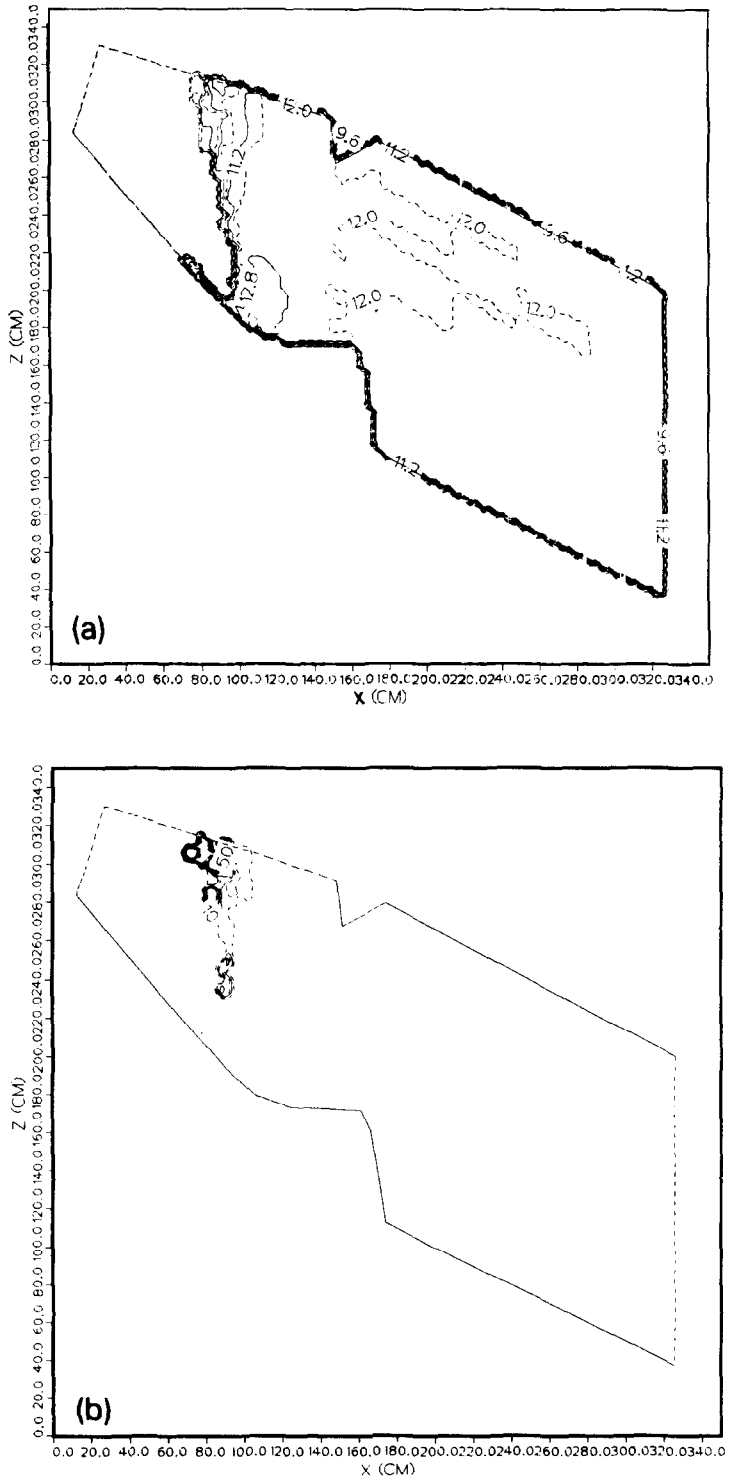

Fig. 5. DEGAS outputs for the reference geometry. (a) Density of D/T atoms (cm^{-3}). (b) Temperature of D/T atoms (eV). (c) Density of molecular D/T (cm^{-3}). (d) Density of He atoms (cm^{-3}) (e) Temperature of He atoms (eV).

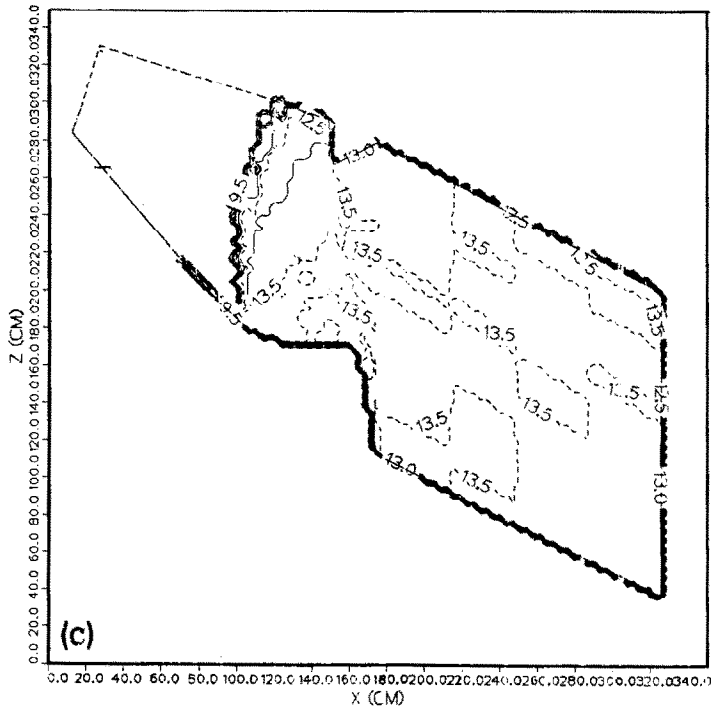

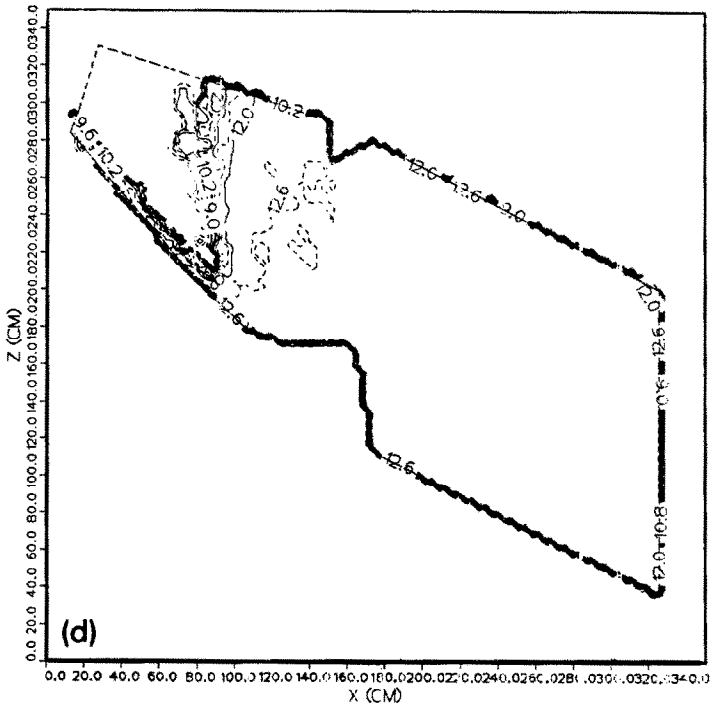

Fig. 5 (continued).

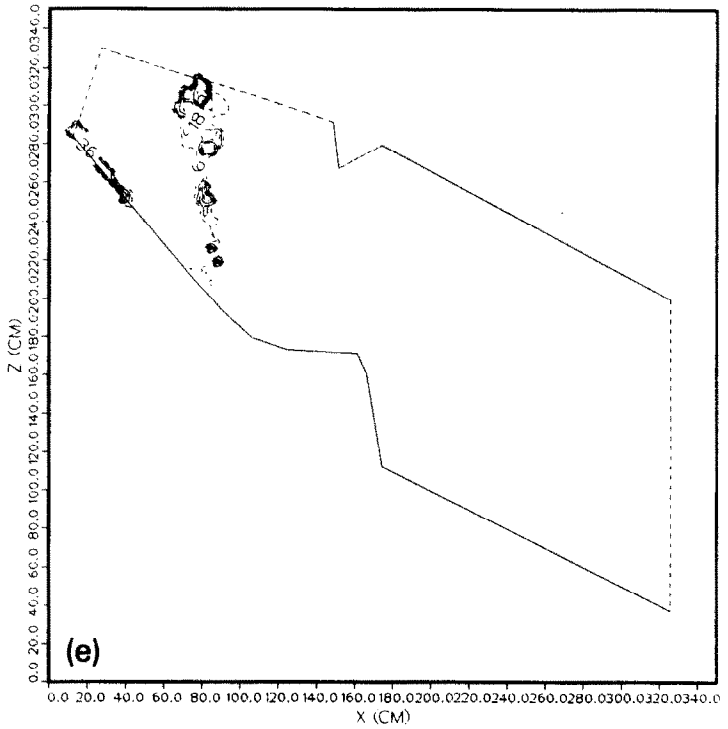

Fig. 5 (continued).

per unit width through an infinitely wide rectangular duct is greater than one with side walls. For the dimensions of ITER this effect should reduce the pumping efficiency of the 2-D (i.e. infinite in the third dimension) simulation by 15% [8]. The as-simulated DEGAS recycling coefficient for the reference case was 0.952. Of 1000 initiated flights, 48 left through the pump openings. If this number is first corrected for 3-D conductance and then for toroidal duct coverage it becomes 0.9898 ± 0.0014. That is, for every 1000 atoms that strike the plate, 10.2 ± 1.4 would leave the device.

Once a match with the B2 code was obtained, seven geometries were simulated. Fig. 4 shows the variations and the two prominent features. The reference case (shown with solid lines), has both a "nose" at the top of the duct entrance and a curved "lip" as part of the divertor plate. Simulations were performed varying the size and combination of these features. All simulations had a pump reflectance of 87.5%. Only 2 of the 16 sections at the end of the duct allowed particles to exit. The other pump boundaries as well as the plasma boundaries were treated as mirrors to all particles. The walls were made of carbon. Any non-reflected atom left the wall as a molecule at the wall temperature. This was taken to be 450°C in the pump duct and higher on the plate, but the exact value had little effect other than determining the average energy of the exiting D/T molecules.

He^{2+} was added to the DEGAS simulation at the same temperature as the D/T^{+}. The density was adjusted to give a flux profile on the divertor plate equal to 0.1 times the D/T profile. For most of the cases presented, the flux profiles were not offset from one another. Though charge exchange between D/T and He is included, neutral-neutral scattering is not. Since neutral atom scattering is very forward peaked [9], the exclusion of this process is not expected to have a large influence on the results. Note that a D/T atom is a hydrogenic species with a mass of 2.5 amu. A D/T molecule has a mass of 5.0 amu.

3. Results

The reference geometry was run on the MFECC Cray 2 "b" machine. A DEGAS run of 1000 D/T flights and 1000 He flights took a total of 197 cpu minutes. The length of the simulation was due to the

Table 1
Effects of altering the divertor throat geometry on the neutral atoms and molecules in the pump duct

Geometry		Average density (10^{13} cm^{-3})			Percentage of D/T exiting as atoms	Average exit energy (eV)		
Nose	Lip	D/T	$(D/T)_2$	He		D/T	$(D/T)_2$	He
no	ref.	0.053	2.23	0.53	13.0	8.3	0.040	0.82
ref.	ref.	0.060	2.94	0.58	30.0	5.3	0.039	1.3
big	ref.	0.021	2.86	0.95	7.0	4.6	0.040	0.65
ref.	small	0.045	2.99	0.63	11.0	10.3	0.039	1.5
no	no	0.089	3.15	0.58	23.0	4.7	0.054	1.1
ref.	no	0.079	3.25	0.63	15.0	4.6	0.055	1.4
big	no	0.055	3.83	0.89	4.0	1.5	0.052	1.4

large geometrical size and paucity of exits. Fig. 5 shows contour plots of the D/T atom density and temperature, D/T molecular density and the He atom density and temperature. The only regions of appreciable atomic temperature is where the density falls markedly due to the presence of the plasma. The spatial variation of the molecules in the pump duct is quite uniform.

Table 1 summarizes the results of varying geometry on the average densities near the end of the pump duct, the percent of the exiting D/T particles that exited as atoms and the average energy of the exiting particles. The standard error for the atomic D/T quantities is roughly 30%. The standard error for the molecular, $(D/T)_2$, quantities is roughly 15%, and the standard error for the He quantities is roughly 10%. In general, as the nose feature is enlarged, the energy of the exiting atoms decreases and the molecular density increases. The nose feature traps some atoms that may have escaped, turning them into molecules. However, those molecules may still have a difficult time making to the exit.

Table 2
Effect of divertor throat geometry on recycling

Geometry		$R_{D/T}$	R_{He}	F
Nose	Lip			
no	ref.	0.962 ± 0.005	0.947 ± 0.007	1.40 ± 0.27
ref.	ref.	0.952 ± 0.007	0.936 ± 0.007	1.33 ± 0.24
big	ref.	0.969 ± 0.007	0.917 ± 0.008	2.67 ± 0.53
ref.	small	0.972 ± 0.005	0.933 ± 0.008	2.39 ± 0.50
no	no	0.953 ± 0.006	0.923 ± 0.008	1.64 ± 0.28
ref.	no	0.948 ± 0.007	0.927 ± 0.008	1.40 ± 0.23
big	no	0.959 ± 0.006	0.904 ± 0.009	2.34 ± 0.41

Table 2 contains the as-simulated recycling coefficients, $R_{D/T}$ and R_{He}. This recycling coefficient, R, is defined as:

$$R = 1 - \frac{\text{number going out pump duct}}{\text{number of ions striking divertor plate}}.$$

Also included in table 2 is the helium pumping enhancement factor. This factor, F, is defined as:

$$F = \frac{1 - R_{He}}{1 - R_{D/T}}$$

and represents the enhancement of helium pumping

Table 3
Effects of shifting the He^{2+} flux profile

Geometry		Shift (cm)	n_{He}(cm^{-3}) $\times 10^{12}$	Average E (eV)	R_{He}	F
Nose	Lip					
ref.	ref.	none	5.8	1.3	0.936 ± 0.007	1.33 ± 0.24
		+20	10.5	1.1	0.851 ± 0.016	3.10 ± 0.54
big	ref.	none	9.5	0.65	0.917 ± 0.008	2.67 ± 0.53
		+20	14.7	0.48	0.865 ± 0.015	4.36 ± 0.90
ref.	no	none	6.3	1.4	0.927 ± 0.008	1.40 ± 0.23
		+20	10.0	1.4	0.853 ± 0.016	2.83 ± 0.47
big	no	none	8.9	1.4	0.904 ± 0.009	2.34 ± 0.41
		+20	14.2	0.73	0.789 ± 0.019	5.15 ± 0.88

over D/T pumping for the same number of particles per unit time striking the divertor plate.

Table 2 shows that helium is always preferentially pumped over D/T. This is largely due to the higher reflection coefficient of He on C at low energies. D/T are more likely to stick to walls and come off as slow molecules. The presence of a nose dramatically increases the chance of He exiting. The total absence of a lip improves the pumping of all species.

The flux profile of He^{2+} on the divertor plate was shifted along the plate toward the duct by 20 cm for four geometries. The results are shown in table 3. Moving the flux outward by this amount markedly decreases R_{He} and increases F for all of the geometries tested.

Acknowledgements

This work was performed under DOE contracts DOE-DEFG-02-89-ER52159 and DE-AC-02-76-CHO-3073. Able assistance was provided to DNR by Daniel Juliano, undergraduate physics major, University of Illinois.

References

[1] International Thermonuclear Experimental Reactor (ITER), Establishment of ITER: Relevant Documents (IAEA, Vienna, 1988).
[2] M.H. Redi and S.A. Cohen, in these Proceedings, J. Nucl. Mater. 176 & 177 (1990).
[3] B. Braams, Eur. Conf. on Controlled Fusion and Plasma Physics, Part II, Budapest, 1985, p. 480.
[4] Summary Report for the January March Joint Work Session 1990, ITER-IL-Ph-5-0-42.
[5] D.B. Heifetz et al., J. Comput. Phys. 46 (1982) 309.
[6] D.N. Ruzic and H.K. Chiu, J. Nucl. Mater. 162–164 (1989) 904.
[7] D.N. Ruzic, Nucl. Instr. and Meth. B47 (1990) 118.
[8] S. Dushman, Scientific Foundations of Vacuum Technique (Wiley, New York, 1949).
[9] D.N. Ruzic, PhD dissertation, Princeton University, 1984.